Identification of a common microdeletion cluster in 7q21.3 subband among patients with myeloid leukemia and myelodysplastic syndrome

Hiroya Asou, Hirotaka Matsui, Yuko Ozaki, Akiko Nagamachi, Megumi Nakamura, Daisuke Aki, and Toshiya Inaba*

Department of Molecular Oncology and Leukemia Program Project
Research Institute for Radiation Biology & Medicine, Hiroshima University, Hiroshima 734-8553, Japan

*Correspondence author. FAX: +81-82-256-7103
E-mail address: tinaba@hiroshima-u.ac.jp (T. Inaba)

ABSTRACT

Monosomy 7 and interstitial deletions in the long arm of chromosome 7 (-7/7q-) is a common nonrandom chromosomal abnormality found frequently in myeloid disorders including acute myeloid leukemia (AML), myelodysplastic syndrome (MDS) and juvenile myelomonocytic leukemia (JMML). Using a short probe-based microarray comparative genomic hybridization (mCGH) technology, we identified a common microdeletion cluster in 7q21.3 subband, which is adjacent to 'hot deletion region' thus far identified by conventional methods. This common microdeletion cluster contains three poorly characterized genes; *Samd9*, *Samd9L*, and a putative gene *LOC253012*, which we named *Miki*. Gene copy number assessment of three genes by real time PCR revealed heterozygous deletion of these three genes in adult patients with AML and MDS at high frequency, in addition to JMML patients. Miki locates to mitotic spindles and centrosomes and downregulation of Miki by RNA interference induced abnormalities in mitosis and nuclear morphology, similar to myelodysplasia. In addition, a recent report indicated Samd9 as a tumor suppressor. These findings indicate the usefulness of the short-probe based CGH to detect microdeletions. The three genes located to 7q21.3 would be candidates for myeloid tumor-suppressor genes on 7q.

Introduction

Monosomy 7 and interstitial deletions in 7q (-7/7q-) are a common nonrandom chromosomal abnormality found frequently in myeloid disorders. In 1964, prior to chromosome band identification, monosomy 7 was first reported in three patients with refractory anemia as monosomy of a C-group chromosome [1]. Since that time, -7/7q- have been identified in 10-20% of a wide range of myeloid malignancies including MDS, AML and JMML [2].

Enormous efforts have been made to identify genes responsible for -7/7q-. In the absence of definitive familial cases, the basic strategy for gene hunting began with identifying patients that carried 7q-. Detailed maps of regions deleted from individual patients were then generated from the results of loss of heterogeneity assays or fluorescence *in situ* hybridization. Unfortunately, the cumulative results from thousands of patients were confounded by the fact that the boundaries of commonly deleted regions derived by separate research groups showed a poor degree of overlap [3]. Currently, it is generally accepted that two or more genes near bands 7q22 and/or 7q34 are involved in myeloid tumors.

Microarray-based comparative genomic hybridization (mCGH) technology allows efficient detection of microdeletions (<100 Kb) that affect one or a few genes, enabling to search for small 7q deletions that are not visible cytogenetically in marrow cells of MDS/AML patients. Initially, bacterial artificial chromosome (BAC)-based mCGH systems were developed, but this system had limited potential to detect microdeletions because of the long probe size (>100 Kb). Thereafter, SNP-array hybridization turned out to be a powerful method for detecting not only single nucleotide polymorphism, but also microdeletions [4]. However, because SNPs tend to cluster within introns and intergenic spaces, SNP-array hybridizations may bias against the detection of microdeletions in critical genes.

Here we describe the application of a modified BAC-based mCGH system that uses short (<10 Kb) genomic DNA fragments without any repetitive sequences as probes to improve the detection of small deletions and reduce background hybridization. Because repeat-free fragments generally overlap exon-containing regions, this type of probe not only yields a high signal/noise ratio, but also can be useful in determining the copy number of a corresponding gene. Using this system for identification of

responsible gene(s) for -7/7q-, we report the isolation of a common microdeletion among JMML patients that contains three poorly characterized genes.

Materials and methods

Short probe-based mCGH. This system was similar to that described by others [5]. Briefly, total 292 repeat-free segments (2.7-9.5 Kb) were identified using BlastN at the NCBI server (235 probes in 7q21.2-7q31.1, 15 in 4q12, 27 in 20q, and 15 in 21q). Each of these fragments was PCR amplified from human placenta DNA (Clontech, Mountain View, CA) and cloned into the pCR-XL-TOPO vector (Invitrogen, Carlsbad, CA). The primer sets used to amplify probes #14 to #16 are listed in Table 1. Sequences of other primer sets are available upon request. Five micrograms of each target DNA, amplified by PCR from each cloned fragment using universal primers in the vector, were printed on poly-L-lysine coated glass slides (Matsunami Glass, Osaka, Japan) using a spotter (SPBIO, Hitachi Software, Tokyo, Japan). Bone marrow samples were obtained after informed consent and approval from the institutional review board at Hiroshima University. Test samples and reference placenta DNA (2.5 μg) were random-prime labeled with CY3- and CY5-dCTP (GE healthcare), respectively, and then hybridized to the slide. Scanning of microarrays was performed using G2505A scanner (Agilent Technologies, Santa Clara, CA) and signals were analyzed with ArrayVision (GE healthcare).

Cell culture and gene transfer. 293 and HeLa(tc) [6] cells were cultured in Dulbecco's modified Eagle medium supplemented with 10% fetal bovine serum (FBS). siRNA oligonucleotides (100 nM, otherwise indicated, Table 2) were transfected using Oligofectamine (Invitrogen). C-terminal FLAG-tagged Mikiα or β protein, or MikiΔN-FLAG(C) protein (lacking N-terminal hydrophobic 30 aa of Mikiβ) was expressed using the pcDNA3 expression vector (Invitrogen).

Other experimental procedures and reagents. Copy number assessment by qPCR was performed according to the procedure described [7]. qRT-PCR was performed as previously described [8], but with HPRT as the internal control. Primer sets used are listed in Table 1. Immunoprecipitation and immunoblot analyses were performed according to standard procedures [9] using 2% gelatin as a blocking agent. Immunostaining and image analyses were performed as described [6; 10]. Rabbit

anti-Miki antibody was raised against GST-Mikiα (aa. 377-462) and affinity purified according to the standard procedures [9].

Results

Identification of three candidate myeloid tumor-suppressor genes in a common microdeletion cluster among JMML patients

Two hundred thirty-five probes in a region spanning 21.7 Mb within 7q21.2-7q31.1 and additional 57 control probes in 4q, 20q, and 21q were applied to a search for microdeletions using a short probe-based mCGH system (see Materials and Methods). Test (leukemia) and reference DNA samples were labeled with CY3- and CY5-dCTP, respectively, and then hybridized to slides on which probes were printed.

We initially selected fresh bone marrow samples from adult AML/MDS patients or DNA from myeloid leukemia cell lines that did not show apparent 7q abnormalities. However, gross regional copy number changes were still detected frequently (Fig. 1A). In addition, 'single copy events', which could include both real copy number changes in a small region and noise of the system, were frequently observed. To test whether this system can detect *bona fide* copy number changes in a small region, we applied this system to genomic DNA extracted from an eosinophilic leukemia cell line, EOL-1, which is known to harbor a deletion spanning 800 Kb between the *Rhe* (*FIP1L1*) gene and the *PDGFα* gene in 4q [11]. All eight probes (#239-#246) that locate within the deletion showed low fluorescence ratios (Fig. 1B, bracket), as well as many single copy events that were also detected in this cell line. We then applied the microarray CGH system to samples from JMML patients, which is a subtype of MDS and is occasionally associated with monosomy 7 [2]. In contrast to adult MDS/AML patients and cell lines, JMML patients mostly carried no gross regional copy number changes nor single copy events (Fig. 1C). However, three contiguous probes (#14-#16) in the 7q21.2-21.3 sub-band were repeatedly found to show a low fluorescence ratio (Fig. 1D). In eight of the 21 JMML patients, at least one of these three probes detected a microdeletion in one allele (Fig. 1E, left), suggesting that a region containing these probes is deleted frequently in JMML.

Three contiguous genes (*Samd9*, *Samd9L* and *LOC253012*) identified by the human genome sequencing consortium (http://www.ncbi.nlm.nih.gov/) were found to overlap probes #14, #15 and #16, respectively (Fig. 2A). This region does not contain

any known copy number polymorphisms (CNPs) [12], nor does it represent any microRNA sequence in miRBase [13] (http://microrna.sanger.ac.uk/).

To confirm the presence of a microdeletion cluster in chromosome 7 of JMML patients, we prepared five primer sets for real-time quantitative PCR analyses (qPCR) that efficiently amplify DNA fragment to allow estimating the copy number of each of these three genes (Fig. 2A) [7]. One allele loss of either one of the three genes was detected in all four patients whose DNA samples were available (Fig. 1E, right). We then extended the qPCR copy number assessment to 65 adult patients with MDS or AML using the five primer sets for the three genes and additional sets for control genes on chromosome 7 and other chromosomes (Fig. 2B). Nearly 30% (19/65) of patients showed loss of one allele in at least one of the three genes, indicating that these three genes are heterozygously deleted at high frequency in both adult and childhood myeloid leukemia. In contrast to the chromosome 7 microdeletions among JMML patients (Fig. 1D), these three genes are more commonly lost with larger deletions in adult MDS/AML patients (Fig. 2C).

Miki-downregulation induced mitotic arrest and abnormal nuclear morphology

Among the three genes, we named a putative gene *LOC253012 Miki* (mitotic kinetics regulator), because of the function of the gene product described below. Candidate *Miki* orthologues were identified in other vertebrates by search of Ensemble Genome Browser (http://www.ensembl.org/index.html), but not in invertebrates, plants, yeast or prokaryotes. Miki transcript was detected on a northern blot as a single 2.6 kb band in kidney and small intestine RNA with very weak signals, suggesting relatively low expression (data not shown). However, two alternatively splicing Miki messages, Mikiα (LOC253012 transcript variant-1, Genbank accession no. NM_001039372) and Mikiβ (variant-2, NM_198151), which are derived from separate first coding exons (1a and 1b, Fig. 2A), were readily amplified by RT-PCR analyses of all examined organs (data not shown). Mikiα and Mikiβ transcripts encode distinctive 26- and 14-amino acid (aa) N-termini, respectively, which precede the same 436-aa C-terminal sequence (Fig. 3A).

Both Miki polypeptides encode three domains suggestive of cell surface proteins: an N-terminal hydrophobic region, a central region homologous to the

immunoglobulin superfamily cell adhesion molecule, and a transmembrane domain-like region. Unexpectedly, immunostaining of HeLa cells using antibodies against the C-terminus of Miki showed an intense signal in the perinuclear region (Fig. 3B, left), which co-localized with Golgi-markers such as Golgin-97 in the interphase (middle). In mitosis, Miki immunostaining localized to centrosomes/spindles (right).

Miki seems to be modified post-translationally in a complex way. Four major bands were detected in immunoblots of 293-cell extracts with anti-Miki antibody (Fig. 3C, lane 1). The migration of the fastest band agreed with the predicted molecular mass (50 kDa). In contrast, transient expression of plasmid pcDNA3-Mikiβ-FLAG(C) generated C-terminal FLAG-tagged Mikiβ proteins that migrated as a broad band between 75 and 95 kDa (lane 2). Because peptide N-glycosidase F (PNGaseF) treatment of immunoprecipitated products from the transfected cells altered the migration of these bands to 50 kDa (lanes 3-5). Treatment of transfected cells with tunicamycin, a glycosylation inhibitor, also shifted the broad band to 50 kDa (lanes 6-7), suggesting that this broad band represents glycosylated forms of Miki. In transfected cells, exogenously expressed Mikiα protein also migrated as a broad band (lane 8); however, expression of MikiΔN-FLAG(C) (which lacks the N-terminal hydrophobic region) produced only one band that migrated slightly faster than p50 (lane 9), suggesting that Miki's N-terminal region functions as a signal peptide. The same blot analyzed with anti-FLAG antibody confirmed the identities of the broad band of exogenous Miki protein (Fig 3D, lanes 2-3, 6, 8), as well as deglycosylated Miki (lanes 5, 7) or MikiΔN protein (lane 9).

Because transient expression of Miki from a variety of virus-derived or eukaryotic promoters resulted uniformly in glycosylated protein, we predict that exogenously expressed Miki is altered by cryptic glycosylation events. In view of these results with Miki overexpression, we applied RNA interference to downregulate endogenous Miki. Six candidate Miki-specific short hairpin RNA (shRNA) sequences were selected and corresponding shRNA-expressing vectors [piGENE-mU6(neo)-hMiki#1 to #6] were prepared. Immunoblot analysis of 293 cells co-transfected with pcDNA3-Mikiβ-FLAG(C) and each one of the six shRNA-expressing vectors demonstrate that three shRNAs (#1, #3, #6) downregulated levels of glycosylated Miki efficiently (Fig. 4A). When cells were transfected with the shRNA-expressing vectors alone, shRNAs expressed from piGENE-mU6(neo)-hMiki#1,

#3 or #6 also downregulated steady-state levels of endogenous Miki p125 and p50 (and p100 and p60 less effectively) (Fig. 4B).

In an alternate experiment, three Miki-based short interference RNAs (siRNAs) reduced steady-state levels of Miki mRNA to varying degrees when transfected directly into 293 cells (Fig. 4C). Immunoblots prepared from these cells showed that the intensities of Miki p125 and p50 signals (and p100 and p60 less effectively) were attenuated within 48 hours of transfection with siRNA#79 or siRNA#80 (Fig. 4D), but not by siRNA#81 and control siRNA. These observations indicated that the p50 represents the unmodified Miki and that p125 could be a post-translationally modified Miki protein, although additional experiments for confirmation are required. Also demonstrated was that siRNA#79 and #80, as well as shRNA#1 efficiently downregulate Miki expression.

To elucidate function of Miki, HeLa cells were treated with siRNAi#80 for 48 hours. Mitotic cells increased from 3% (control siRNA-treated cells) to 12%, suggesting that Miki-downregulation causes mitotic arrest. As expected, Miki staining decreased significantly in cells treated with siRNA#80 (Fig. 4E, left and middle), and showed disorganized spindle formation (middle). Hoechst 33342 staining revealed scattered chromosomes (middle), which is clearly distinguishable from normal prometaphase by wide and irregular distribution of chromosomes. These abnormal prometaphases were observed in 15 to 43% of mitotic cells treated with either siRNA#79 or siRNA#80 (Fig. 4E, right). In contrast, cells treated with control siRNA rarely (<2%) showed scattered chromosomes. Miki-downregulation also affects nuclear morphology. Cultures of HeLa cells which stably expressed shRNA#1 frequently (approximately 20%) contained more than two nuclei (Fig. 4F, left).

Scattered chromosomes in mitosis and bi- or tri-nucleated cells are routinely observed in MDS and related AML (MDS/AML) as a part of myelodysplasia (Fig. 4F, middle and right panels), suggesting that Miki-downregulation may contribute to these abnormal mitosis and nuclear morphology in MDS/AML. To test this hypothesis, mRNA levels of Miki in bone marrow cells from MDS or AML patients were estimated by real-time qRT-PCR. Expression levels of Miki was significantly ($P<0.05$) lower in leukemia cells with myelodysplasia to compare with those without apparent myelodysplasia (Fig. 4G).

Discussion

Here we identified a microdeletion cluster among JMML patients within 120 kb in 7q21.3 subband. This cluster contains three poorly characterized genes: *Miki (LOC253012)*, *Samd9* and *Samd9L*. Since single gene deletion of *Samd9* or *Miki* was proved by two independent methods (mCGH and qPCR) in patient #1 or #8, respectively, we prefer to consider that three genes, rather than one of them, are candidates for myeloid tumor-suppressors on 7q. Three genes are also deleted in adult MDS and AML either as a part of large deletions or single gene loss (Fig. 2C).

Among systems detecting microdeletions, SNP-array hybridization becomes the first choice for primary screening [4]. However, because SNPs tend to cluster within introns and intergenic spaces, SNP-array may not always be the best. For instance, although there are 9 SNP probes in this microdeletion cluster in Genome-Wide SNP6.0 system (Affymetrix), no probes can detect *Samd9* gene deletion (Fig. 2A, bottom). In addition, only one probe (A-866741) locates to coding region, casting doubt on the potential of SNP-array to detect small deletions in the critical genes. Application of the short probe-based mCGH to samples containing few copy number abnormalities (such as JMML) would be a good alternative of SNP-array.

In myeloid tumors, -7/7q- has been most implicated in pathogenesis of MDS, which is characterized by myelodysplasia (morphological abnormality in hematopoietic progenitors)[2]. Myelodysplasia includes abnormal nuclear morphologies, such as bi-, tri- or multi-nucleated cells and abnormal mitoses involving lagging chromosomes, multi-polar mitoses or so-called colchicine-mitosis (chromosome scattering similar to colchicine-treated cells). Despite the fact that these features are routinely observed, underlying molecular mechanisms are largely unknown. Our findings (Figs. 4E to 4G) raised a possibility that low levels expression of Miki plays important roles in myelodysplasia, although detailed mechanisms remained to be established.

Samd9 and Samd9L are related proteins with 60% amino acid identity. Recently, point mutations of Samd9 was reported as a causative gene alterations in Normophosphatemic Familial Tumoral Calcinosis, a rare autosomal recessive disorder in five families of Jewish-Yemenite origin [14; 15]. In addition, downregulation of Samd9 was reported to be implicated in aggressive fibromatosis [16], suggesting that Samd9 could be a tumor suppressor. However, Samd9/Samd9L do not show

significant homology to any other genes and no biological functions were elucidated. We overexpressed or downregulated Samd9 or Samd9L in various human cells and found no prominent phenotypes, possibly because functional redundancy of these two proteins. Because there is only *Samd9L* gene in mouse genome [16], *Samd9L*-deficient mice would show unambiguous phenotypes. Indeed, currently we are accumulating phenotypes from *Samd9L*-deficient mice that support our hypothesis that Samd9/Samd9L are myeloid tumor-suppressors.

Acknowledgements

We thank Drs. S. Kojima, R. Hanada, M. Kobayashi K. Koike and T. Kyo for providing sample. This work was supported by Grants-in-Aid for Scientific Research from the Ministry of Education, Culture, Sports, Science and Technology of Japan.

Figure legends

Fig. 1. Detection of microdeletions. (A-D) Profiles of short probe-based mCGHs. Normalized average fluorescence ratios by control placenta DNA (Y-axis) were derived from three replicates for each probe (X-axis). AML cell lines, MUTZ-3 (A) and EOL-1 (B), which shows reduced signals from 8 probes located in a 4q12 microdeletion (bracket); arrows indicate isolated copy number changes. JMML patients #15 (C) and #1 (D); an arrow shows reduced signals with probe #16. (E) Deletion profile summary for eight JMML patients using microarray CGH probes #11 to #18 (left) and qPCR primer sets #1 to #5 (right). Black boxes indicate a deletion in one allele. NA: samples not available.

Fig. 2. Isolation of *Samd9, Samd9L and Miki*. (A) A map of 7q21.3. The relative locations of exons for the three genes are depicted as boxes with coding exon numbers above. The positions of probes used in mCGH (#14 to #16) and primer sets used for qPCR (#1 to #5) are shown below. The positions of SNP probes in a SNP array system (Genome-Wide SNP6.0) are also shown (bottom). (B) Percent of patients with adult MDS/AML who lack one allele of each of the genes indicated in the diagram to the left. Results of qPCR study. (C) Deletion profile summary of qPCR data from adult MDS/AML patients. Unless otherwise indicated below, each column of boxes corresponds to results from one patient. Black boxes indicate a deletion in one allele.

Fig. 3. Expression and localization of Miki. (A) Diagram of *Miki* gene structure. The initiation codon for Mikiα or Mikiβ is located in exon 1a or 1b, respectively. The Mikiα transcript is spliced using a cryptic splice acceptor in exon 1b. Exons 1a and 1b both encode *in frame* stop codons (tga) upstream of the initiation codons. The 5' ends of exons 1a and 1b have not yet been determined. (B) Immunostaining of HeLa cells with Miki (FITC) and Golgin-97 (PE). lnterphasic (left and middle), and mitotic cells (right). (C-D) Immunoblot analysis using Miki (C, top), FLAG (D, top) or β-actin (bottom) antibodies. Lane 1, untreated 293 cells; lane 2, cells transfected with pcDNA3-Mikiβ-FLAG(C); lane 3, anti-FLAG immunoprecipitates of cells transfected with pcDNA3-Mikiβ-FLAG(C); lanes 4-5, anti-FLAG immunoprecipitates incubated for 1 hour in the absence or presence of PNGaseF; lane 6-7, cells transfected with

pcDNA3-Mikiβ-FLAG(C) cultured in the absence or presence of tunicamycin (1 μg/ml); lane 8-9, cells transfected with pcDNA3-Mikiα-FLAG(C) or pcDNA3-MikiΔN-FLAG(C).

Fig. 4. Miki downregulation by RNAi. (A) Immunoblot analysis using FLAG (top) or β-actin (bottom) antibodies: lane 1, lysate from untreated 293 cells; lanes 2 to 9, cells transfected with pcDNA3-Mikiβ-FLAG(C) with shRNA-expressing vectors for six candidate Miki-based shRNA (lanes 2 to 7) or empty shRNA-expressing vector (lane 8). (B) Immunoblot analysis of HeLa(tc) cells transfected with shRNA-expressing vectors for six candidate Miki-based shRNA (lanes 1 to 6), or an empty shRNA-expressing vector (V; lane 7). Lysates from untreated 293 cells (lane 8). (C) Miki mRNA expression levels in 293 cells treated with control siRNA, siRNA#79, #80 or #81 for 48 hours are expressed as percent signal (measured using qRT-PCR) relative to an untreated control. The mean and SD for four independent experiments. (D) 293 cells were either untreated (lane 1) or transfected with control siRNA (lane 2), siRNA#79 (lanes 3), siRNA#80 (lane 4 at 40 nM), or siRNA#81 (lanes 5). (E) Immunostaining with Miki antibody of mitotic HeLa(tc) cells treated with control siRNA or siRNA#80 (48 hrs). DNA was stained with Hoechst 33342 (left and middle). Percentages of mitosis with scattered chromosomes in 200 mitotic cells (right). (F) Giemsa staining of HeLa cells expressing Miki shRNA#1 (left) and mitotic bone marrow cells of a MDS patient (middle and right). (G) Miki transcripts analyzed by qRT-PCR and normalized by HPRT in MDS/AML with (n=20) or without (n=17) myelodysplasia. Vertical short lines indicate average.

References

[1] E.J. Freireich, J. Whang, J.H. Tjio, R.H. Levin, G.M. Brittin, and I.E. Frei, Refractory anemia, granulocytic hyperplasia of bone marrow, and a missing chromosome in marrow cells. A new clinical syndrome? . Clinical Res. 12 (1964) 284.

[2] E.S. Jaffe, N.L. Harris, H. Stein, and J.M. Vardiman, Pathology and genetics of tumours of haematopoietic and lymphoid tissues, IARC press, Lyon, France, 2001.

[3] R. Todd, B. Bia, E. Johnson, C. Jones, and F. Cotter, Molecular characterization of a myelodysplasia-associated chromosome 7 inversion. Br J Haematol 113 (2001) 143-52.

[4] A. Dutt, and R. Beroukhim, Single nucleotide polymorphism array analysis of cancer. Curr Opin Oncol 19 (2007) 43-9.

[5] K.K. Mantripragada, I. Tapia-Paez, E. Blennow, P. Nilsson, A. Wedell, and J.P. Dumanski, DNA copy-number analysis of the 22q11 deletion-syndrome region using array-CGH with genomic and PCR-based targets. Int J Mol Med 13 (2004) 273-9.

[6] N. Oshimori, M. Ohsugi, and T. Yamamoto, The Plk1 target Kizuna stabilizes mitotic centrosomes to ensure spindle bipolarity. Nat Cell Biol 8 (2006) 1095-101.

[7] R. Weksberg, S. Hughes, L. Moldovan, A.S. Bassett, E.W. Chow, and J.A. Squire, A method for accurate detection of genomic microdeletions using real-time quantitative PCR. BMC Genomics 6 (2005) 180.

[8] R. Kuribara, H. Honda, H. Matsui, T. Shinjyo, T. Inukai, K. Sugita, S. Nakazawa, H. Hirai, K. Ozawa, and T. Inaba, Roles of Bim in apoptosis of normal and Bcr-Abl-expressing hematopoietic progenitors. Mol Cell Biol 24 (2004) 6172-83.

[9] T. Shinjyo, R. Kuribara, T. Inukai, H. Hosoi, T. Kinoshita, A. Miyajima, P.J. Houghton, A.T. Look, K. Ozawa, and T. Inaba, Downregulation of Bim, a proapoptotic relative of Bcl-2, is a pivotal step in cytokine-initiated survival signaling in murine hematopoietic progenitors. Mol Cell Biol 21 (2001) 854-64.

[10] N. Tokai-Nishizumi, M. Ohsugi, E. Suzuki, and T. Yamamoto, The chromokinesin Kid is required for maintenance of proper metaphase spindle size. Mol Biol Cell 16 (2005) 5455-63.

[11] J.H. Griffin, J. Leung, R.J. Bruner, M.A. Caligiuri, and R. Briesewitz, Discovery of a fusion kinase in EOL-1 cells and idiopathic hypereosinophilic syndrome. Proc Natl Acad Sci U S A 100 (2003) 7830-5.

[12] J. Sebat, B. Lakshmi, J. Troge, J. Alexander, J. Young, P. Lundin, S. Maner, H. Massa, M. Walker, M. Chi, N. Navin, R. Lucito, J. Healy, J. Hicks, K. Ye, A. Reiner, T.C. Gilliam, B. Trask, N. Patterson, A. Zetterberg, and M. Wigler, Large-scale copy number polymorphism in the human genome. Science 305 (2004) 525-8.

[13] S. Griffiths-Jones, R.J. Grocock, S. van Dongen, A. Bateman, and A.J. Enright, miRBase: microRNA sequences, targets and gene nomenclature. Nucleic Acids Res 34 (2006) D140-4.

[14] O. Topaz, M. Indelman, I. Chefetz, D. Geiger, A. Metzker, Y. Altschuler, M. Choder, D. Bercovich, J. Uitto, R. Bergman, G. Richard, and E. Sprecher, A deleterious mutation in SAMD9 causes normophosphatemic familial tumoral calcinosis. Am J Hum Genet 79 (2006) 759-64.

[15] I. Chefetz, D. Ben Amitai, S. Browning, K. Skorecki, N. Adir, M.G. Thomas, L. Kogleck, O. Topaz, M. Indelman, J. Uitto, G. Richard, N. Bradman, and E. Sprecher, Normophosphatemic familial tumoral calcinosis is caused by deleterious mutations in SAMD9, encoding a TNF-alpha responsive protein. J Invest Dermatol 128 (2008) 1423-9.

[16] C.F. Li, J.R. MacDonald, R.Y. Wei, J. Ray, K. Lau, C. Kandel, R. Koffman, S. Bell, S.W. Scherer, and B.A. Alman, Human sterile alpha motif domain 9, a novel gene identified as down-regulated in aggressive fibromatosis, is absent in the mouse. BMC Genomics 8 (2007) 92.

Figure 1

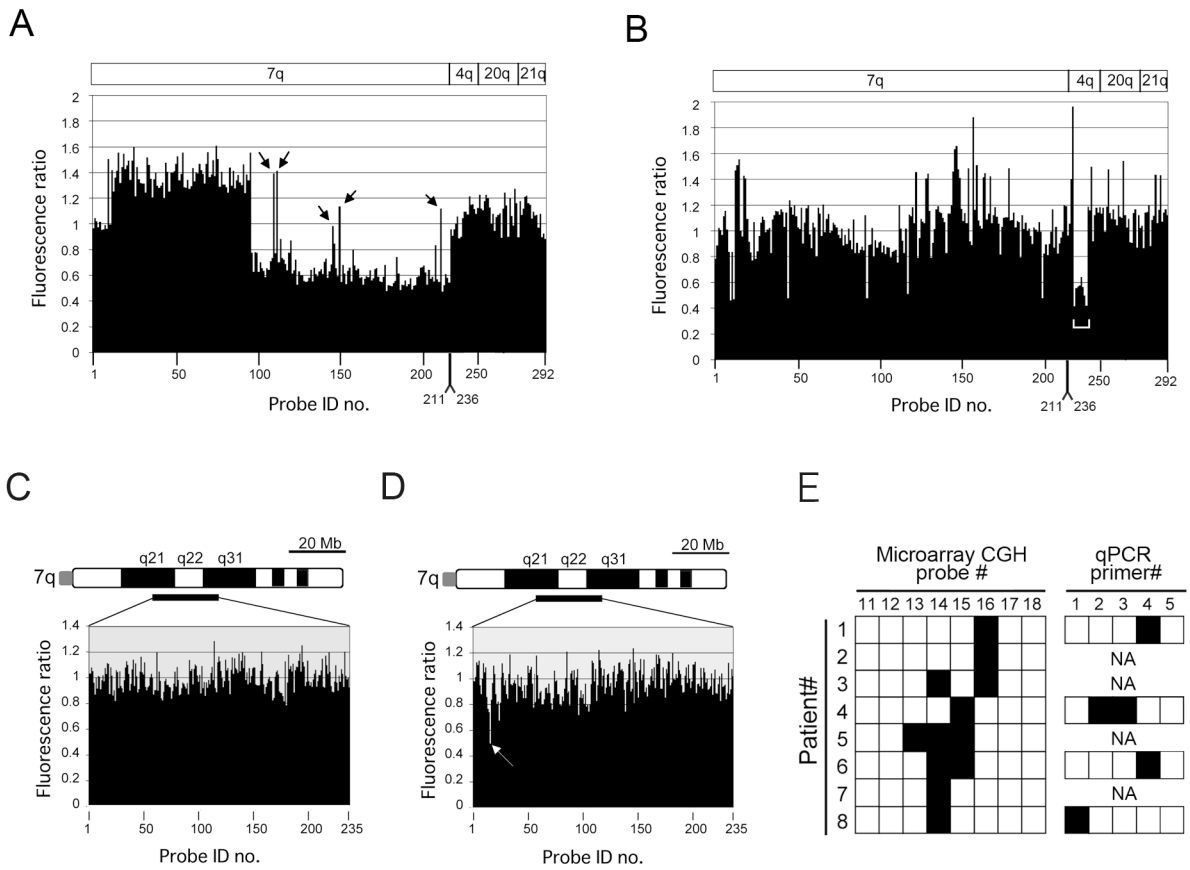
A
7q
4q
20q
21q
Fluorescence ratio
Probe ID no.
211
236
B
7q
4q
20q
21q
Fluorescence ratio
Probe ID no.
211
236
C
20 Mb
7q
q21
q22
q31
Fluorescence ratio
Probe ID no.
D
20 Mb
7q
q21
q22
q31
Fluorescence ratio
Probe ID no.
E
Microarray CGH probe #
11 12 13 14 15 16 17 18
qPCR primer#
1 2 3 4 5
Patient#
1
2
3
4
5
6
7
8
NA
NA
NA
NA

Figure 2

A

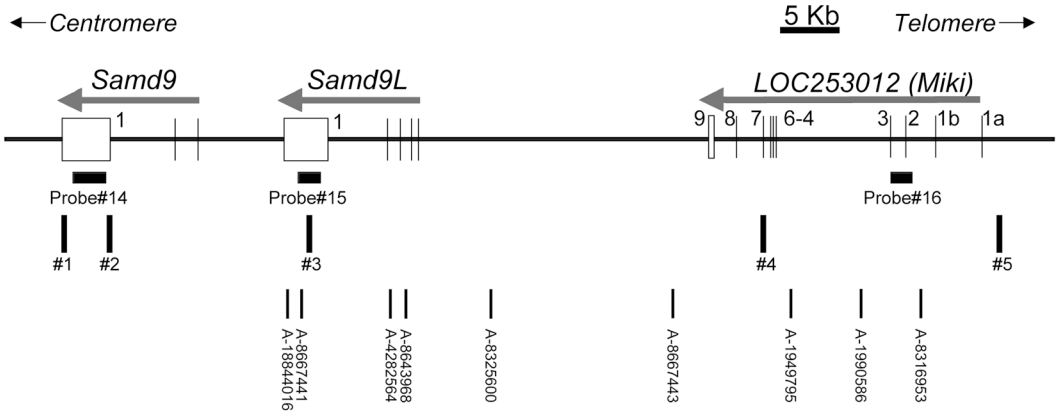
Centromere
5 Kb
Telomere
Samd9
Samd9L
LOC253012 (Miki)
1
1
9
8
7
6-4
3
2
1b
1a
Probe#14
Probe#15
Probe#16
#1
#2
#3
#4
#5
A-8667441
A-18844016
A-8643968
A-4282564
A-8325600
A-8667443
A-1949795
A-1990586
A-8316953

B

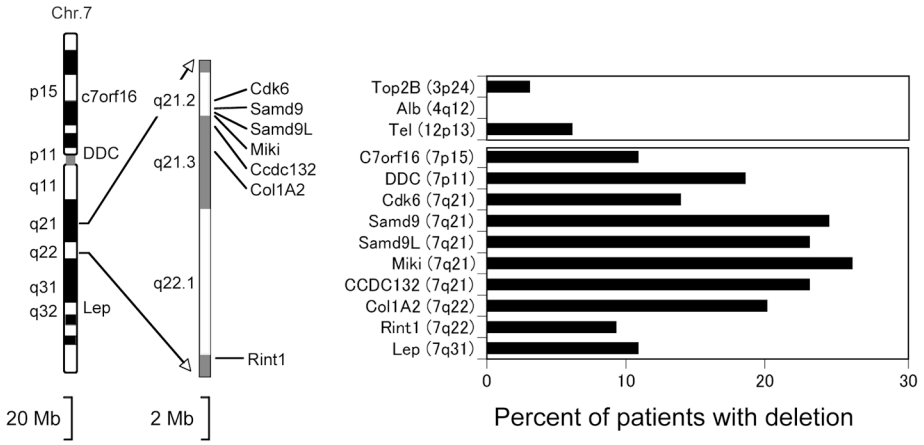
Chr.7
p15
c7orf16
p11
DDC
q11
q21
q22
q31
q32
Lep
q21.2
q21.3
q22.1
Cdk6
Samd9
Samd9L
Miki
Ccdc132
Col1A2
Rint1
20 Mb
2 Mb
Top2B (3p24)
Alb (4q12)
Tel (12p13)
C7orf16 (7p15)
DDC (7p11)
Cdk6 (7q21)
Samd9 (7q21)
Samd9L (7q21)
Miki (7q21)
CCDC132 (7q21)
Col1A2 (7q22)
Rint1 (7q22)
Lep (7q31)
0
10
20
30
Percent of patients with deletion

C

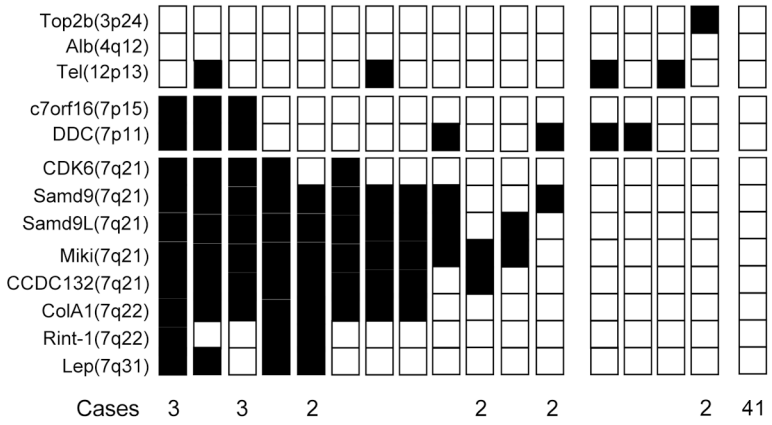
Top2b(3p24)
Alb(4q12)
Tel(12p13)
c7orf16(7p15)
DDC(7p11)
CDK6(7q21)
Samd9(7q21)
Samd9L(7q21)
Miki(7q21)
CCDC132(7q21)
ColA1(7q22)
Rint-1(7q22)
Lep(7q31)
Cases
3
3
2
2
2
2
41

Figure 3

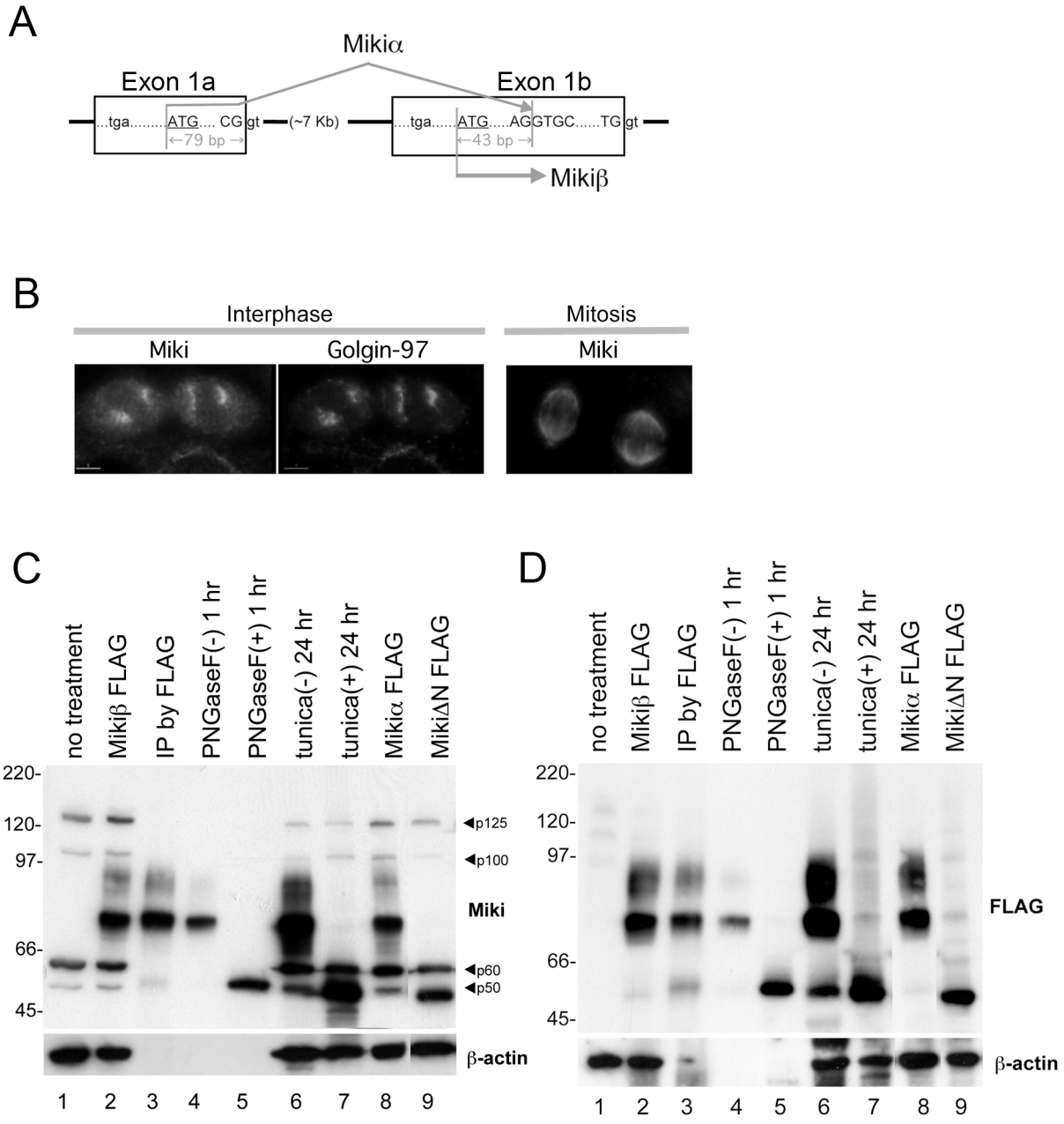
A
Mikiα
Exon 1a
Exon 1b
...tga.....ATG.... CG gt
(~7 Kb)
....tga.....ATG.....AGGTGC.....TG gt
←79 bp →
←43 bp →
Mikiβ
B
Interphase
Mitosis
Miki
Golgin-97
Miki
C
no treatment
Mikiβ FLAG
IP by FLAG
PNGaseF(-) 1 hr
PNGaseF(+) 1 hr
tunica(-) 24 hr
tunica(+) 24 hr
Mikiα FLAG
MikiΔN FLAG
220-
120-
97-
66-
45-
◀p125
◀p100
Miki
◀p60
◀p50
β-actin
1 2 3 4 5 6 7 8 9
D
no treatment
Mikiβ FLAG
IP by FLAG
PNGaseF(-) 1 hr
PNGaseF(+) 1 hr
tunica(-) 24 hr
tunica(+) 24 hr
Mikiα FLAG
MikiΔN FLAG
220-
120-
97-
66-
45-
FLAG
β-actin
1 2 3 4 5 6 7 8 9

Figure 4

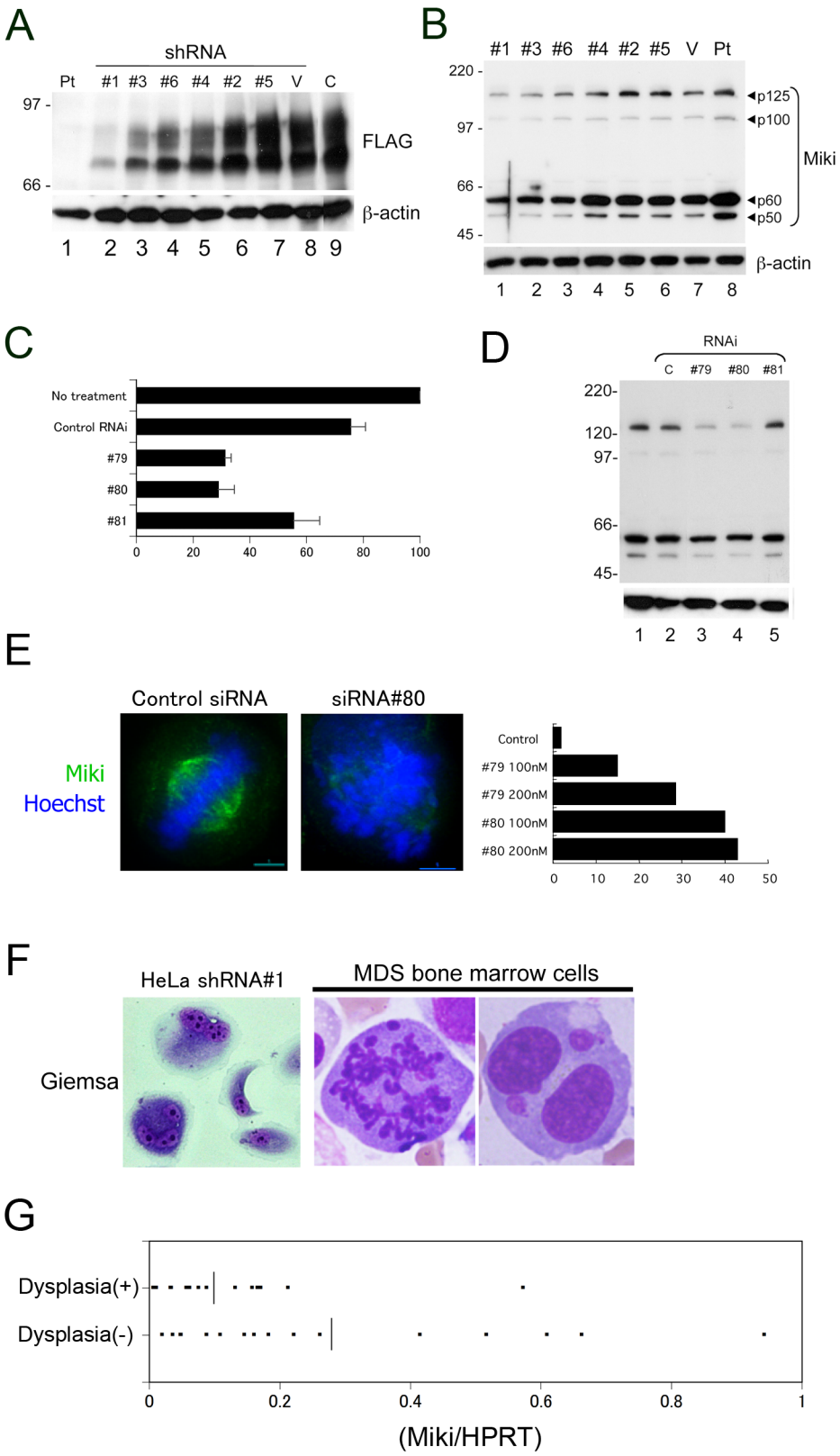
A
shRNA
Pt #1 #3 #6 #4 #2 #5 V C
97 -
66 -
FLAG
β-actin
1 2 3 4 5 6 7 8 9
B
#1 #3 #6 #4 #2 #5 V Pt
220 -
97 -
66 -
45 -
p125
p100
p60
p50
Miki
β-actin
1 2 3 4 5 6 7 8
C
No treatment
Control RNAi
#79
#80
#81
0 20 40 60 80 100
D
RNAi
C #79 #80 #81
220-
120-
97-
66-
45-
1 2 3 4 5
E
Control siRNA
siRNA#80
Miki
Hoechst
Control
#79 100nM
#79 200nM
#80 100nM
#80 200nM
0 10 20 30 40 50
F
HeLa shRNA#1
MDS bone marrow cells
Giemsa
G
Dysplasia(+)
Dysplasia(-)
0 0.2 0.4 0.6 0.8 1
(Miki/HPRT)